Turbulence and Intermittent Transport in Magnetized Plasmas

Jens Juul Rasmussen, Odd Erik Garcia, Volker Naulin, and Anders H. Nielsen

`jens.juul.rasmussen@risoe.dk`

Association EURATOM-Risø National Laboratory,
Department of Optics and Plasma Research
OPL-128 Risø, DK-4000 Roskilde, Denmark

Motivation

Cross field transport of particles and heat in magnetically confined plasmas is dominated by anomalous - turbulent transport!

In the edge/scrape-off-layer (SOL) region transport is strongly intermittent and characterized by:

- large-amplitude, radially propagating blob-like structures of particles and heat, generated close to the last closed flux surface (LCFS),
- resulting in asymmetric conditional wave forms, and skewed and flattened PDFs,
- results in localized power loads at PFCs.

Motivation

Cross field transport of particles and heat in magnetically confined plasmas is dominated by anomalous - turbulent transport!
In the edge/scrape-off-layer (SOL) region transport is strongly intermittent and characterized by:

- large-amplitude, radially propagating blob-like structures of particles and heat, generated close to the last closed flux surface (LCFS),
- resulting in asymmetric conditional wave forms, and skewed and flattened PDFs,
- results in localized power loads at PFCs.

Observed under a variety of conditions:

see, e.g., Zweben Phys. Fluids **28** 974 (1985) Antar *et al*, PoP **10** 419 (2003); Boedo *et al*, PoP **10**, 1670 (2003); Zweben *et al*, Nucl. Fus. **44**, 134 (2004); Grulke *et al* PoP **13**, 012306 (2006); Garcia *et al* PPCF **48**, L1 (2006)

Density blob observations

Observations of density blobs at the outboard midplane of ALCATOR C-mod (D_α - light)

O. Grulke *et al.* PoP **13**, 012306 (2006).

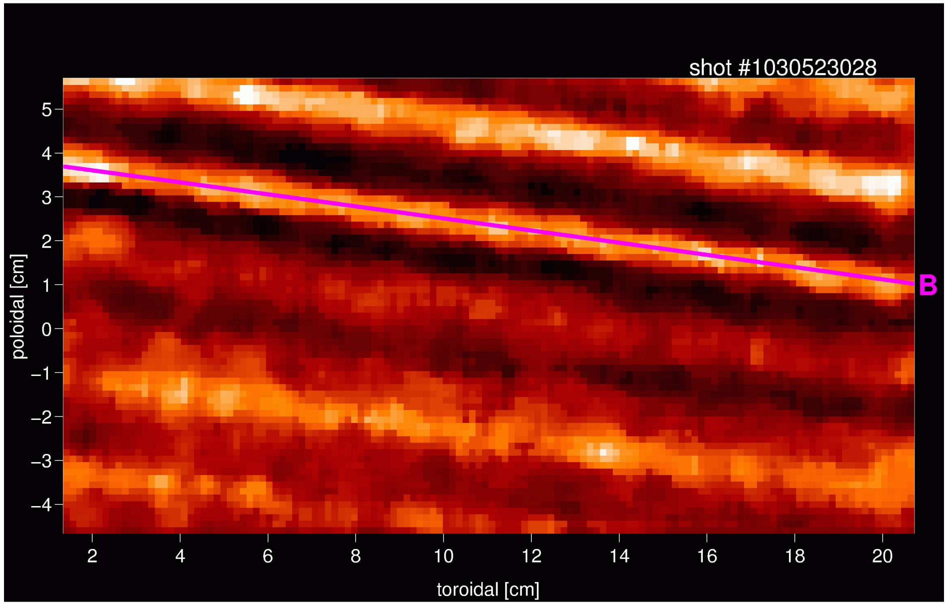

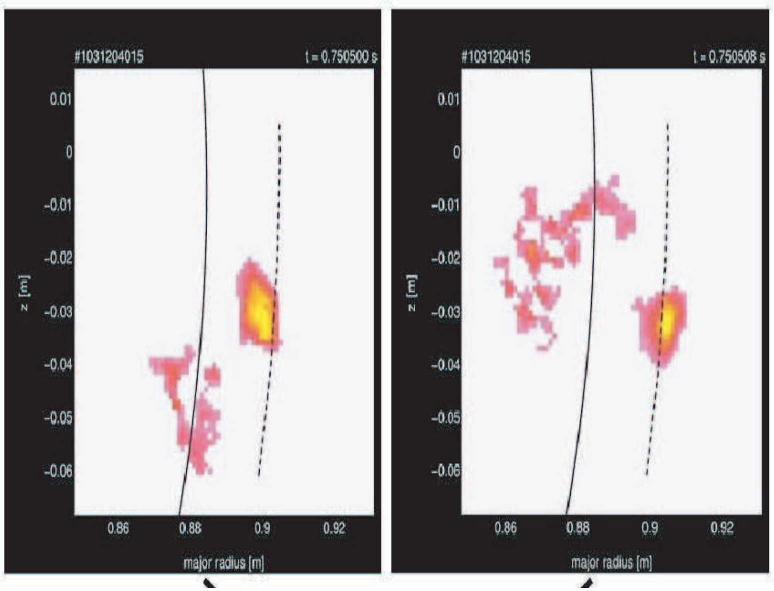

Structure along B.

Radial propagation, $V \approx 0.05c_s$.

Density blob theory

Several recent works:

Krasheninnikov PLA **283**, 268 (2001)

Curvature drift: charging of a density blob → radial propagation, velocity fraction of c_s, linear model, no self-consistent blob formation

D'Ippolito *et al*, PoP **9**, 222 (2002)
Bian *et al*, PoP **10**, 671 (2003)
D'Ippolito *et al*, CPP **44**, 205 (2004)
Garcia *et al*, PoP **12**, 090701 (2005)
Garcia *et al*, PoP **13**, in press (2006)

Similar mechanism for uprising density bubbles in ionospheric E-F layer – inverse stratification in a gravitational field.

e.g. Ott JGR **83**, 4369 (1978); Fejer and Kelley Rev. GSP **18**, 401 (1080)

Blob propagation mechanism

Charge separation by curvature drift:

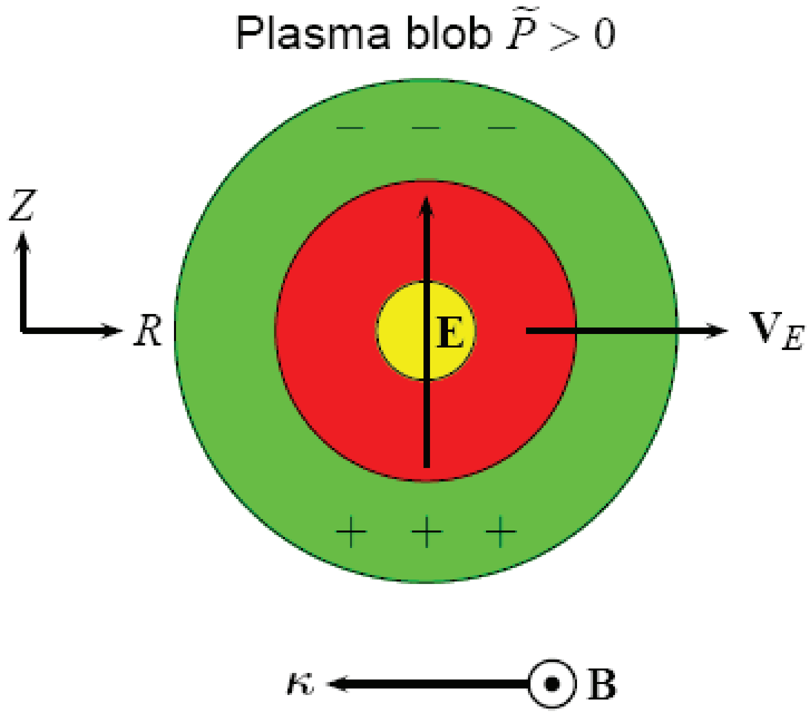

$$\kappa = (\mathbf{b} \cdot \nabla)\mathbf{b}$$

Density blob propagation

Garcia *et al*, PoP **12**, 090701 (2005),

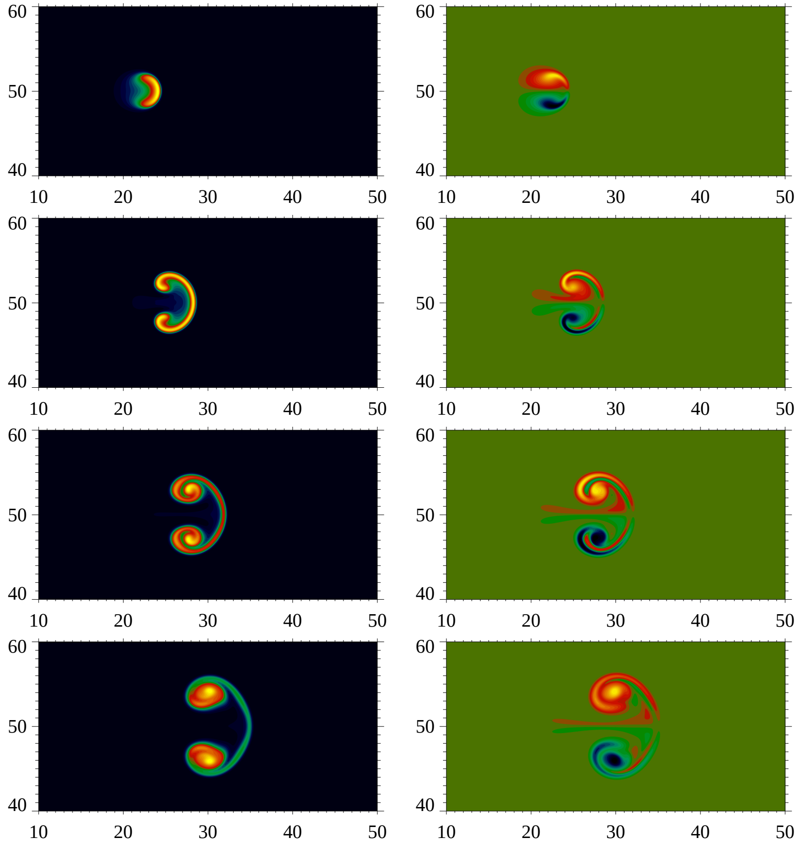

Density and vorticity (“charge”) evolution. Initial Gaussian density blob.

Radial velocity: $v/c_s \leq (2\Delta l/R\Delta n/n_0)^{1/2} \approx 0.2$

Turbulence Model : ESEL

A self-consistent description of fluctuations and intermittent transport in the edge/SOL by employing the RISØ ESEL (Edge SOL Electrostatic) model for interchange dynamics that:

- include separate plasma production “edge” and loss region “SOL”,
- allow self-consistent flows and profile relaxations,
- profiles and fluctuations are NOT separated,
- conserve particles and energy in collective dynamics.

Results agree very well with experimental observations, e.g., TCV, Lausanne (Garcia *et al* PPCF **48**, L1 (2006)) and JET (Naulin et al IAEA-2006)

Garcia, Naulin, Nielsen, Rasmussen, PRL **92** 165003 (2004); PoP **12**, 090701 (2005); Physica Scripta **T122**, 89 (2006).

Geometry and Coordinates

We consider the outboard midplane of a toroidal plasma

The non-uniform magnetic field is $\mathbf{B} = -(B_0 R_0/R)\widehat{\Theta}$, described in elementary cylindrical coordinates (R, Θ, Z).

Applying a local slab approximation: $x = R - R_a$, $y = Z$-poloidal coordinate, $z = -\Theta$.

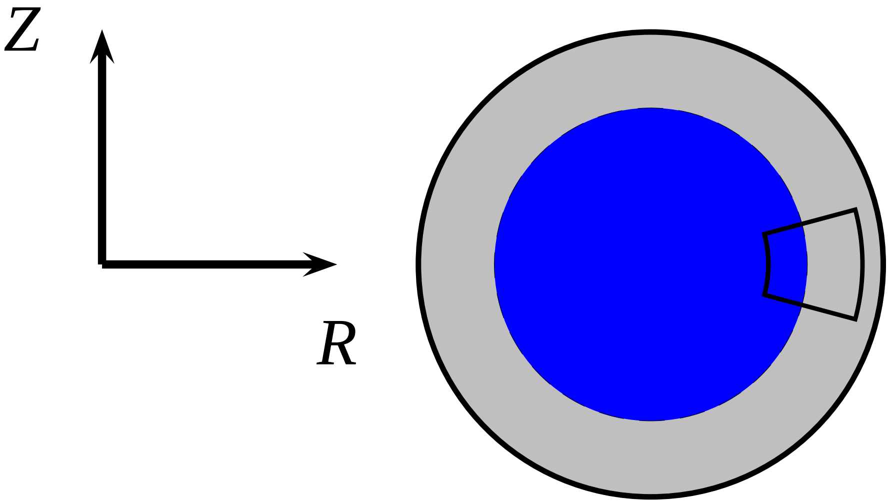

Model Equations

Fluid model cold ions and quasi-neutrality

$$\frac{dn}{dt} + n\mathcal{C}(\phi) - \mathcal{C}(nT) = \nu_n \nabla_\perp^2 n - \sigma_n (n-1) + S_n,$$

$$\frac{dT}{dt} + \frac{2T}{3}\mathcal{C}(\phi) - \frac{7T}{3}\mathcal{C}(T) - \frac{2T^2}{3n}\mathcal{C}(n) = \nu_T \nabla_\perp^2 T - \sigma_T (T-1) + S_T,$$

$$\frac{d\Omega}{dt} - \mathcal{C}(nT) = \nu_\Omega \nabla_\perp^2 \Omega - \sigma_\Omega \Omega, \quad \Omega = \nabla_\perp^2 \phi.$$

Advective derivative and curvature operators defined by

$$\frac{d}{dt} = \frac{\partial}{\partial t} + \frac{1}{B}\widehat{\mathbf{z}} \times \nabla\phi \cdot \nabla, \quad \mathcal{C} = \nabla\left(\frac{1}{B}\right) \cdot \widehat{\mathbf{z}} \times \nabla, \quad B(x) = \frac{1}{1+\varepsilon+\zeta x}.$$

Conservation of particles and global energy (lowest order in ζ)

$$E(t) = \int d\mathbf{x} \left[\frac{1}{2}\left(\nabla_\perp \phi\right)^2 + \frac{3}{2} nT \right].$$

Instability, Energy Integrals

Interchange instability: $N = -B'(p_0' - \frac{5}{3}B') \leq 0$ instability at low field side.

Naulin et al. PRL **81**, 4148 (1998); PoP **10**, 1075 (2003)

Define the kinetic energy of the fluctuating and poloidal mean motions,

$v_0(x,t) = \frac{1}{L_y}\int_0^{L_y} v_y(\mathbf{x},t)dy = \partial\phi_0/\partial x$:

$$K(t) = \int \frac{1}{2}\left(\nabla_\perp\widetilde{\phi}\right)^2 d\mathbf{x}, \qquad U(t) = \int \frac{1}{2} v_0^2\, d\mathbf{x}\ .$$

Energy Transfer, Transport

Define the kinetic energy of the fluctuating and poloidal mean motions,
$v_0(x,t) = \frac{1}{L_y}\int_0^{L_y} v_y(\mathbf{x},t)dy = \partial\phi_0/\partial x$:

$$K(t) = \int \frac{1}{2}\left(\nabla_\perp\widetilde{\phi}\right)^2 d\mathbf{x}, \qquad U(t) = \int \frac{1}{2} v_0^2\, d\mathbf{x}\ .$$

Energy transfer rates from thermal energy to the fluctuating motions, and from the fluctuating to the poloidal mean flow:

$$F_p(t) = \int pC(\phi)\, d\mathbf{x}, \qquad F_v(t) = \int \widetilde{v}_x\widetilde{v}_y \frac{\partial v_0}{\partial x}\, d\mathbf{x}.$$

F_p is also a measure of the turbulent energy transport.

Simulation Geometry

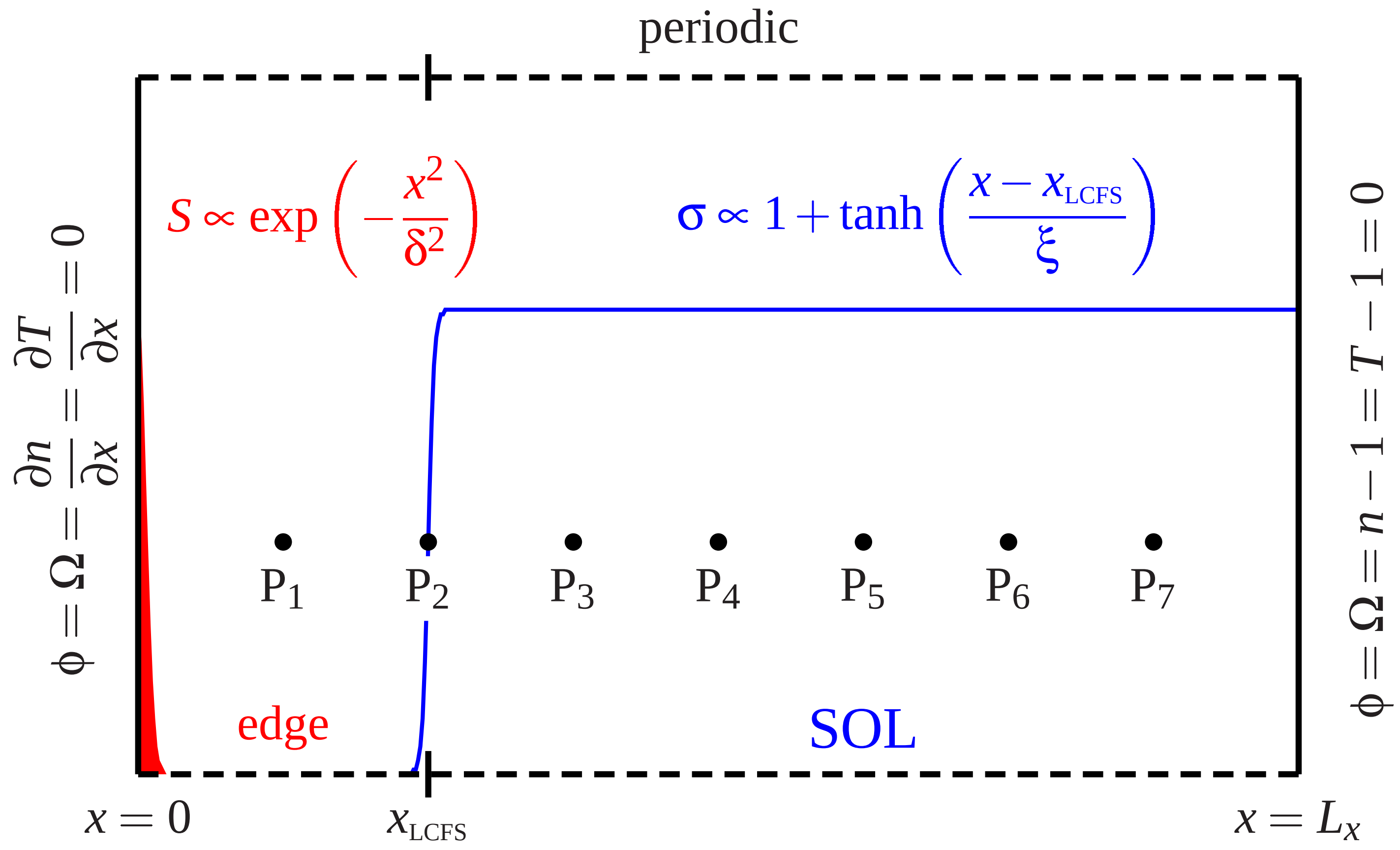

Domain $L_x = 2L_y = 200$, resolution 512×256, $x_{\text{LCFS}} = 50$. SOL damping rates $\sigma_n = \sigma_\Omega = \sigma_T/5 = 3\zeta/2\pi q$ with $q = 3$; magnetic curvature $\varepsilon = 0.25$, $\zeta = 5 \times 10^{-4}$; collisional diffusion $\nu = 10^{-2}$; timespan 4×10^6

Density Evolution

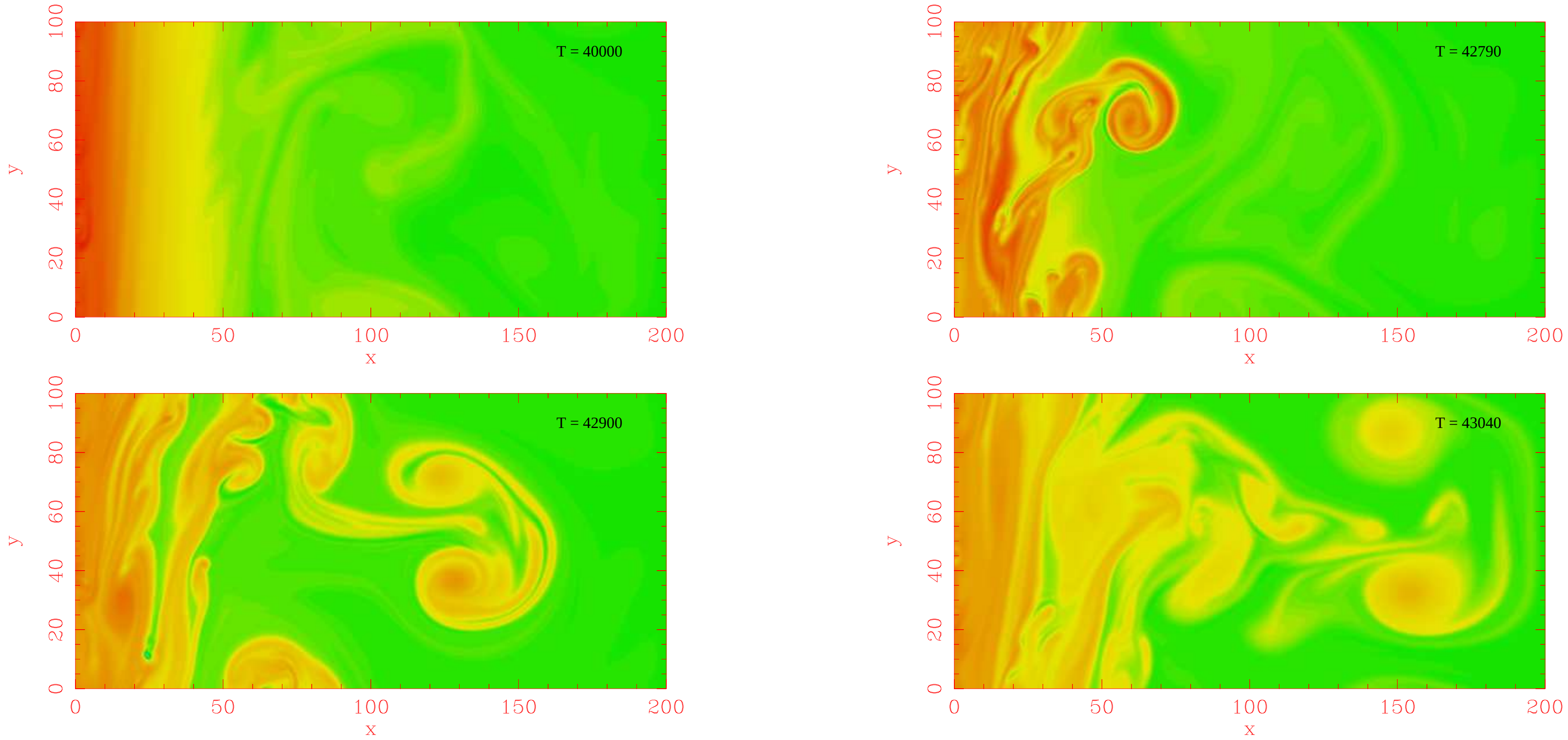

Density blob propagation: The blob is generated inside LCFS ($x_{LCFS} = 50$). Radial propagation velocity of the structures is estimated to $\approx 0.05c_s$; but with large variance. Envisage the density blob as a filament elongated along the magnetic field with a ballooning structure.

Density Evolution

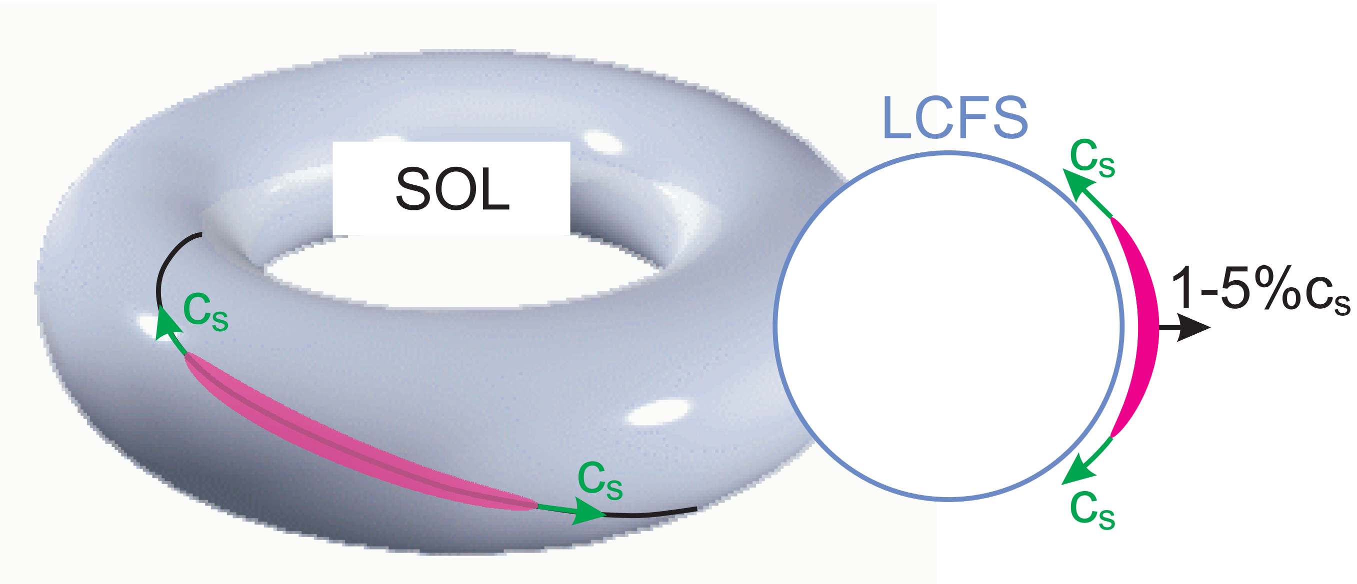

Density blob propagation: The density blob as a filament elongated along the magnetic field with a ballooning structure.

Energy Transfer

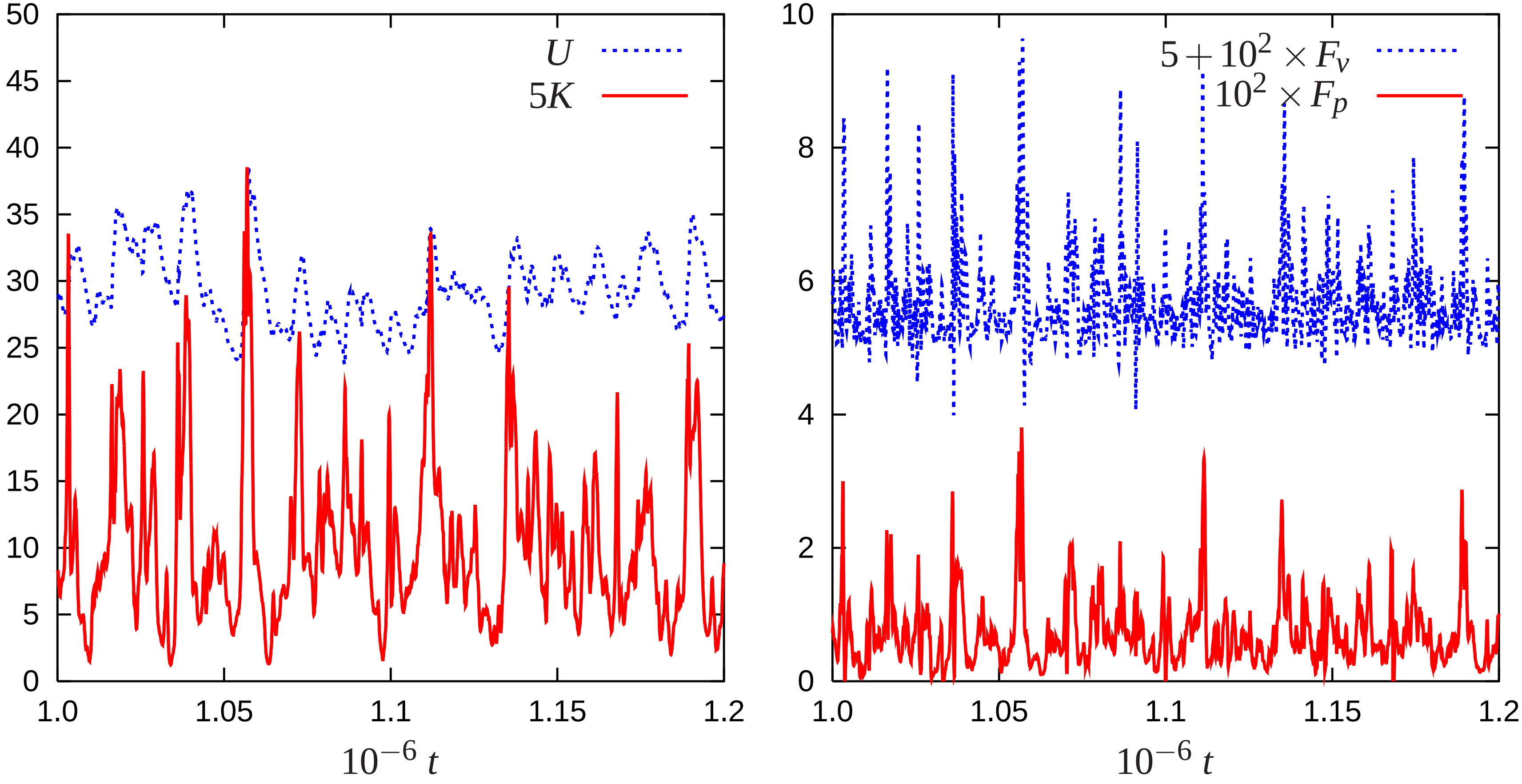

Bursting : Kinetic energy contained by the mean U *and fluctuating* K *motions and the collective energy transfer terms* F_p *and* F_v *.*

Energy Transfer

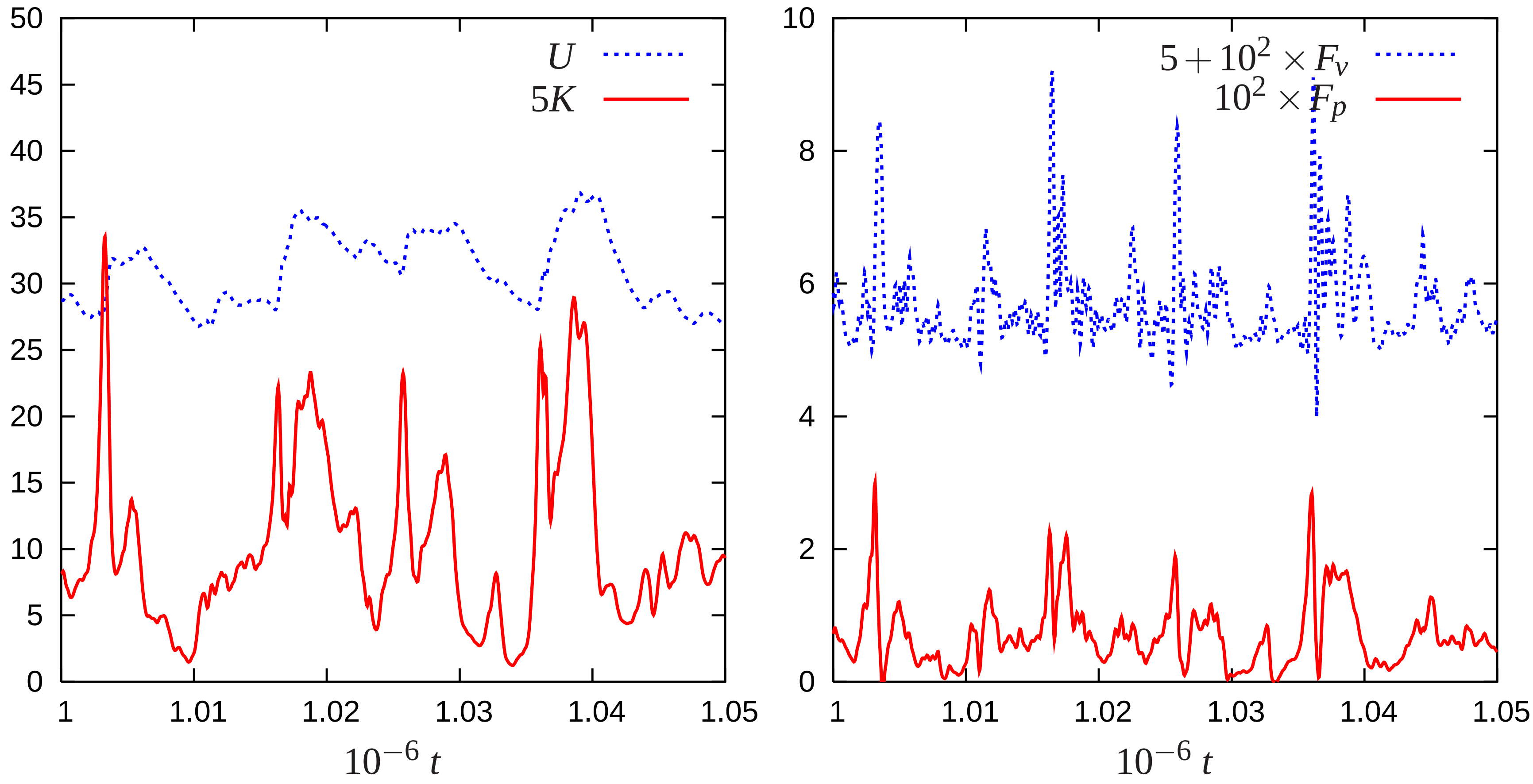

Bursting : Expanded time scale, $(\nu = 10^{-2})$ *.*

Energy Transfer

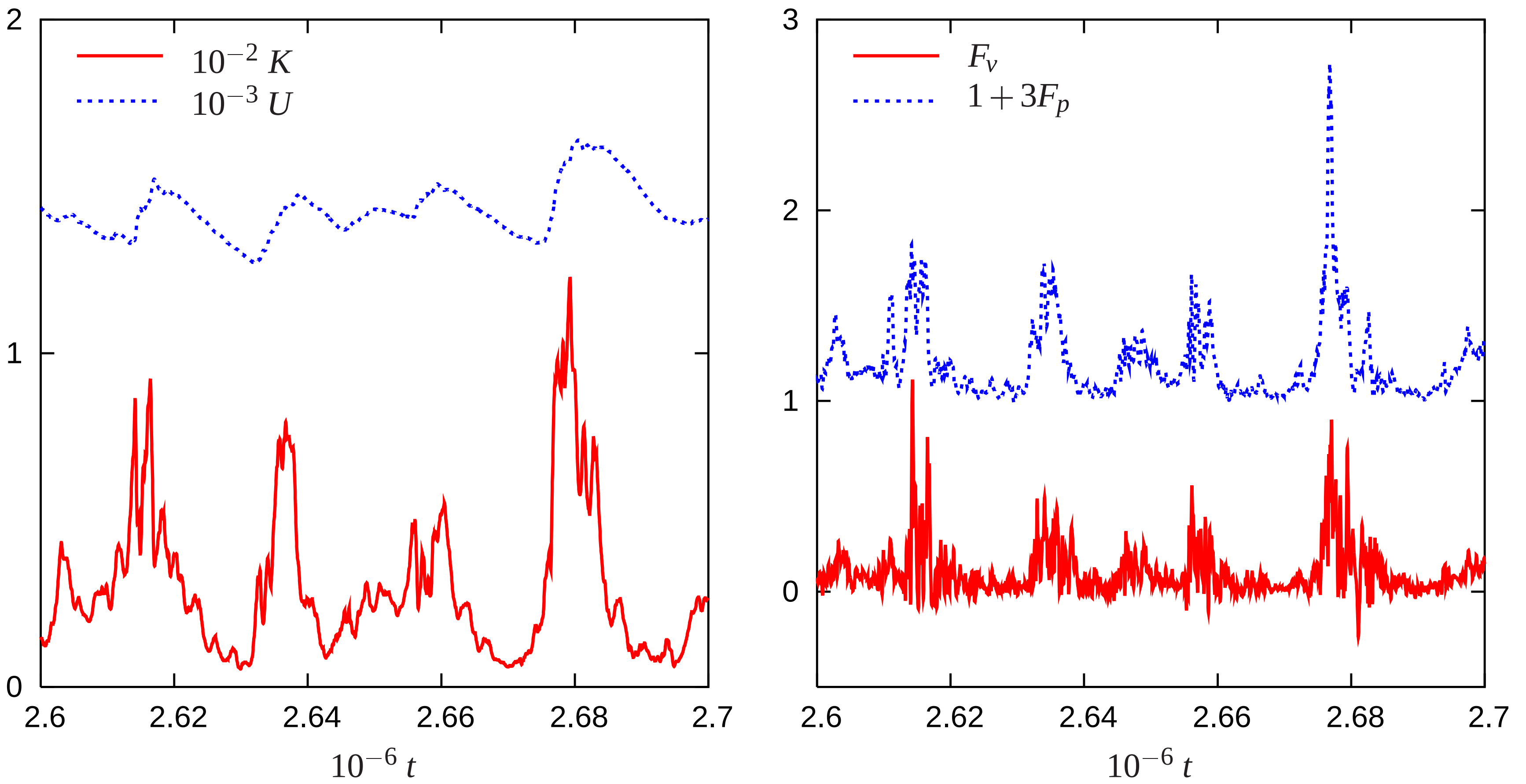

Bursting : Half viscosity $\nu = 5 \times 10^{-3} \rightarrow$ *double time span*

Robust behavior

Energy flow

- Instability drive in the edge
- Turbulence propagating into the SOL
- Saturates and via particle and momentum fluxes
- Profile modification and flow generation; weak transport
- Shear flow stabilizes the instability (Benilov *et al* Phys. Fluids **14** 1674 (2002))
- Profile steepening, flow damping (viscous timescale)
- Instability drive

Bursting period related to viscous timescale.

Density fluctuations

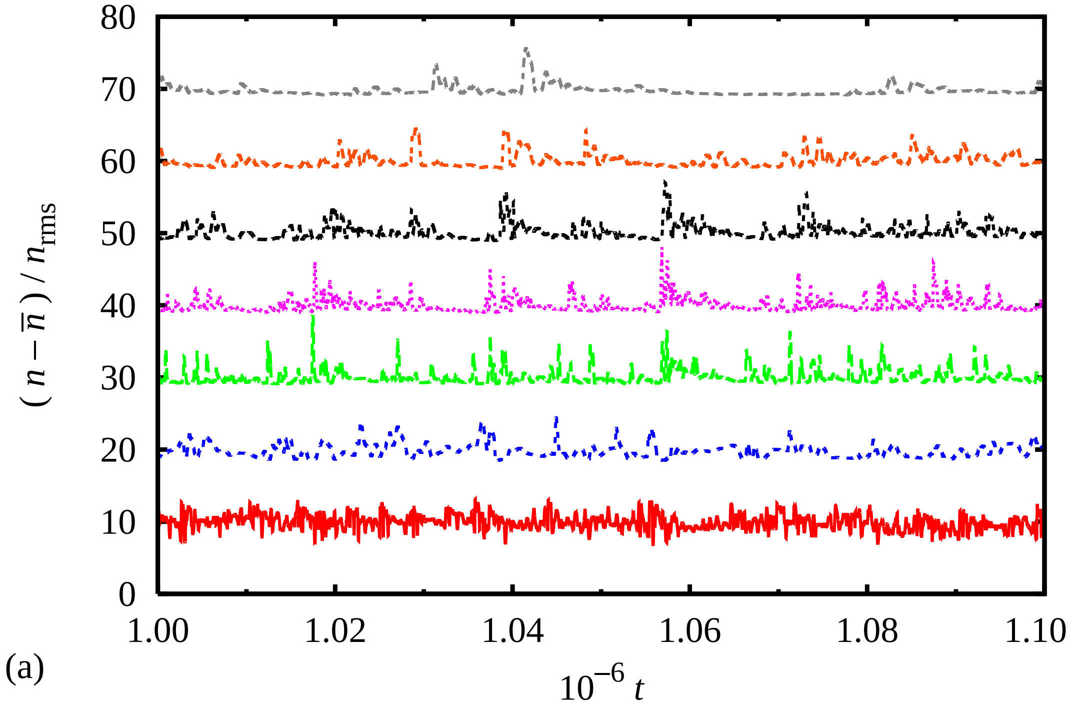

Temporal evolution of the particle density as recorded by the probes P_i.

Spatial Structure

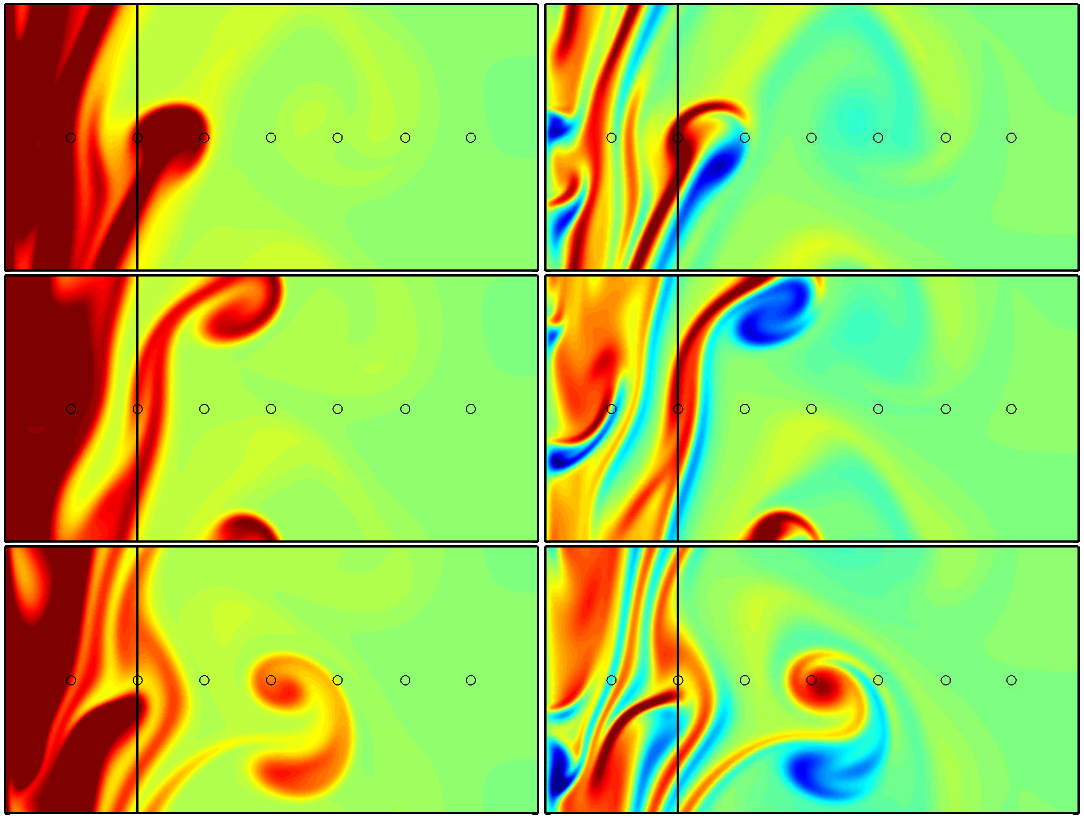

Particle density (left) and vorticity (right) during a burst ($\Delta t = 500$)

Single-Point PDFs

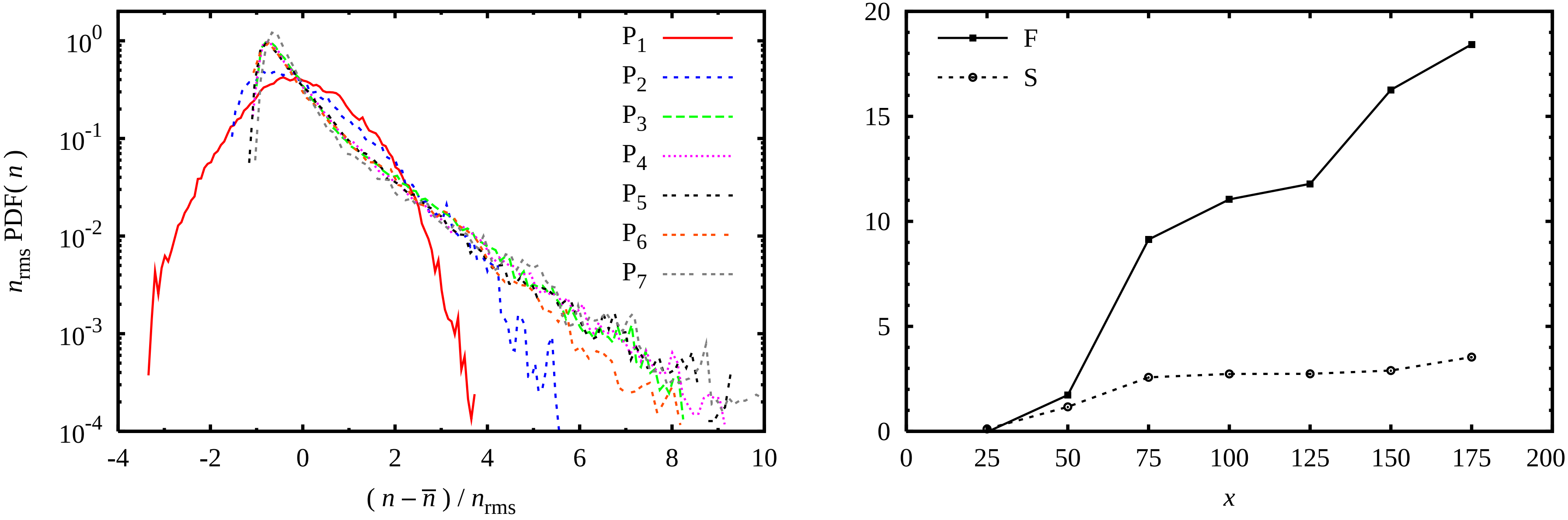

Scaled probability density distribution functions, PDF, of density fluctuations at P_i. $i > 2$ *exponential tails, indicating strong blob structures. Skewness,* S *and flatness,* F, *factors for the density fluctuations*

Single-Point PDFs

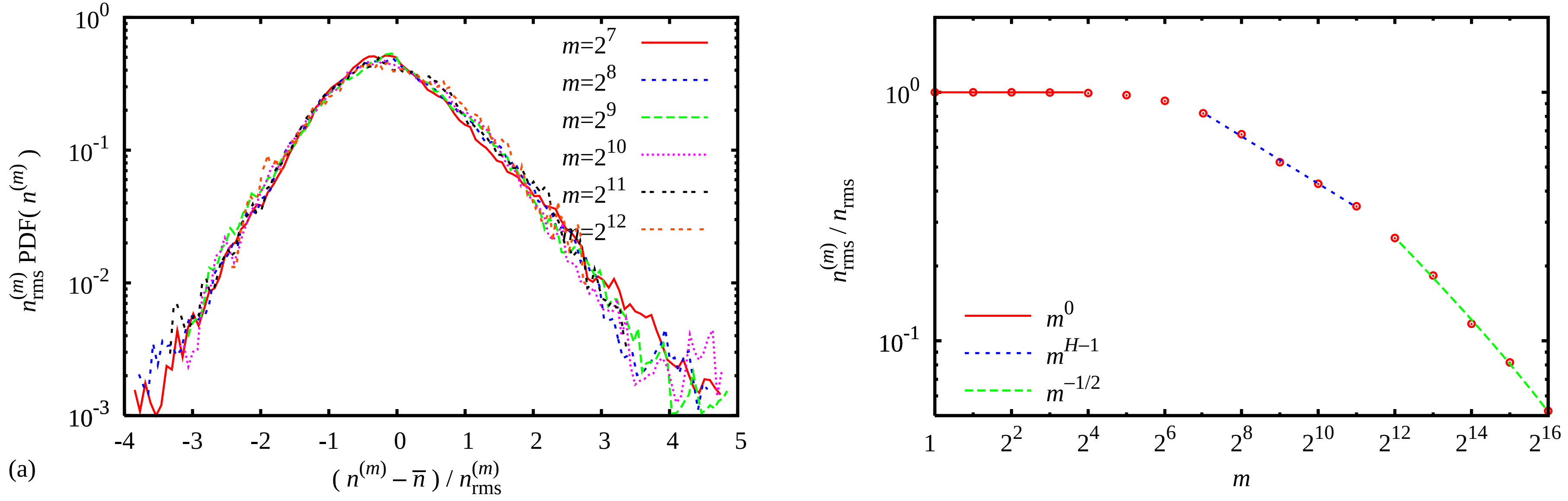

Coarse grained PDF for density fluctuations at P_3. m number of points in coarse graining. Self-similarity for scales up to $m = 2^{12}$ ($\tau \approx 10^4$).

Scaling with m, for mesoscales: $H = 0.68$ revealing long range correlations.

For long scales $m \geq 2^{12}$ ($\tau > 10^4$) $H = 0.5$ uncorrelated random noise.

Particle Density Flux

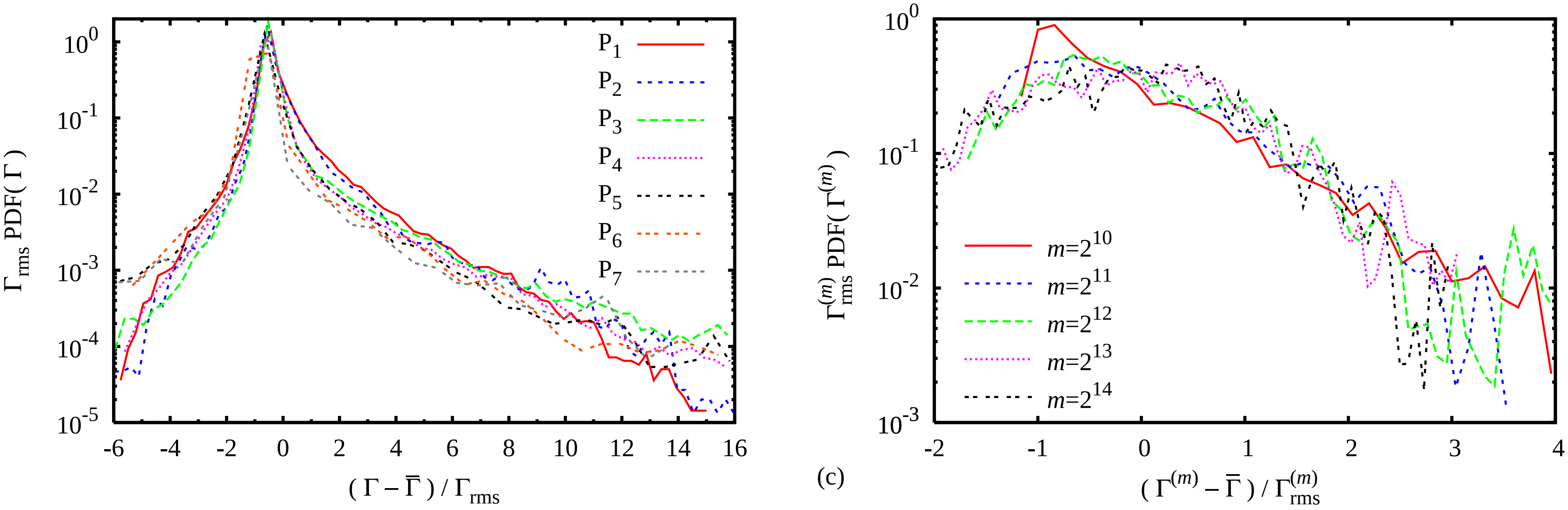

Re-scaled PDF of particle density flux, $\Gamma = (n - \overline{n})v_x$, *measured at the probes,* P_i. *Exponential tails: flux dominated by strong bursts.*

Coarse grained PDF at P_3: *Self-similarity for for mesoscales with* $H = 0.5$.

Particle Density Flux

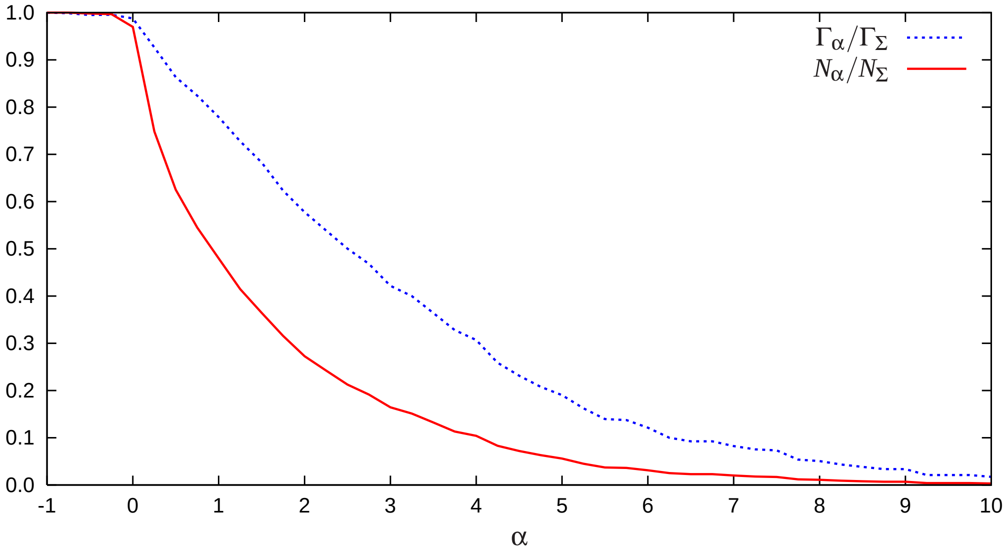

Conditional particle flux $\Gamma_\alpha = \langle \Gamma_0 | \Gamma_0 - \bar{\Gamma}_0 > \alpha \Gamma_{0rms} \rangle$ *relative to total flux* Γ_Σ *at* P_3*.*

Relative count number N_α *of sub-records.*

Few events contain most of the flux. Burst rate $\propto$ *viscosity.*

Transport characterized by the Flux PDF; not diffusive: find the “unique PDF“

Prediction of loads to divertor plates and PFC.

Effective Diffusion?

Transport modelling: linear combination of effective convection and diffusion

$$\Gamma = nV_{\text{eff}} - D_{\text{eff}}\frac{\partial n}{\partial r} \quad\Rightarrow\quad \frac{\Gamma}{n} = V_{\text{eff}} - D_{\text{eff}}\frac{1}{n}\frac{\partial n}{\partial r}.$$

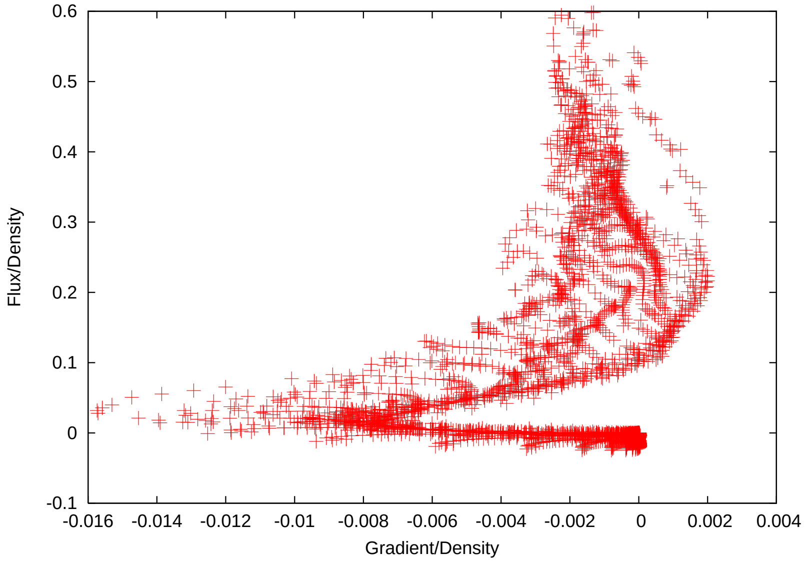

Scatter plot for the flux–gradient relation.

Transport cannot be parameterized by an effective particle diffusivity and a convective velocity

Conclusions ...

The non-linear dynamics of interchange turbulence (2-D ESEL-code) yields very good agreement with experimental measurements:

- the formation of blobs due to profile relaxations,
- radial propagation velocities around 0.1 acoustic speed,
- asymmetric wave forms; skew and flat PDFs,
- intermittent transport,
- cannot be parameterized by an effective diffusion coefficient and an effective convection velocity,
- lead to localized in space and time power loads on PFCs.

Experiment Comparison

Experimental results from TCV-Tokamak, Lausanne: excellent quantitative agreement:
Garcia *et al* PPCF **48**, L1 (2006)

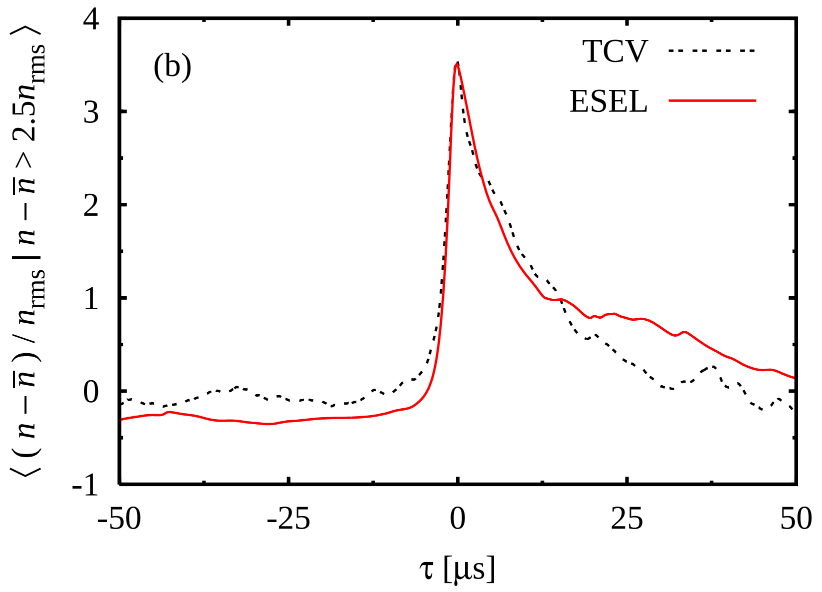

Conditional averaged density blob

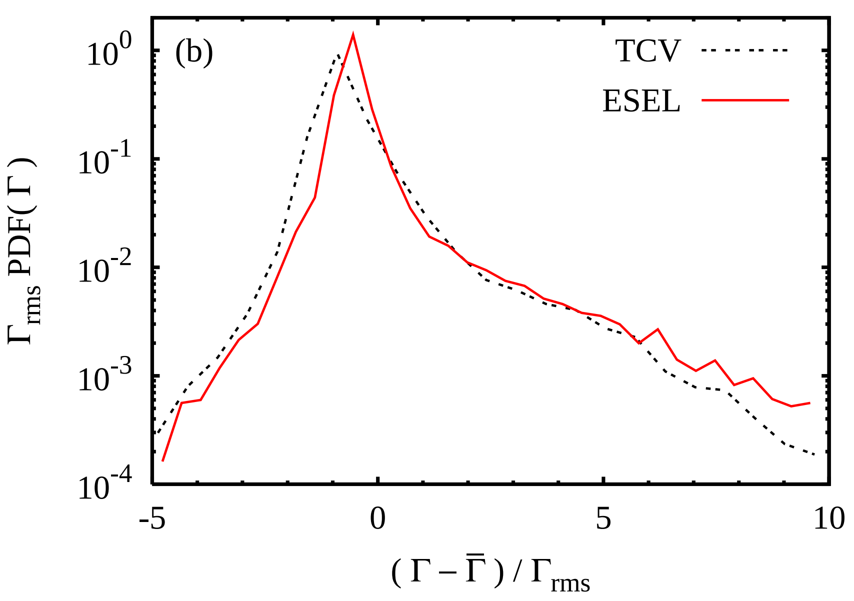

PDF of the particle density flux

.... and Outlook

More complete modelling of edge and SOL turbulence

- should be 3-D, non-local, and energy-conserving,
- with geometry effects and sheath boundary conditions,
- finite ion temperature: GESEL,
- address the relation to ELMs.

Blobs in Hot Plasmas

Finite ion temperature: Gyrofluid model GESEL;
(J. Madsen, J. Staerk *et al.*, EPS-2006, Rome, Italy)

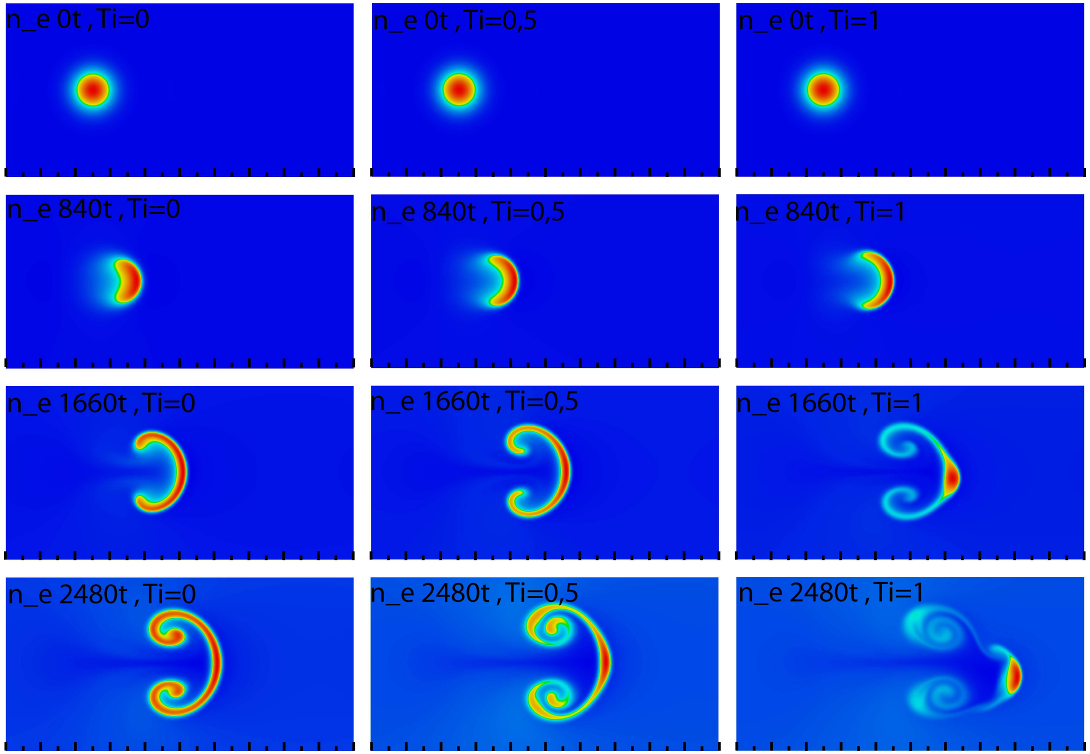

Impurity Dynamics

Impurity dynamics are modeled by tracing passive particles convected by the turbulent field.
Assumptions: Impurity density low, fully ionized, cold.

Impurity convection: $\frac{d\vec{x}}{dt} = \vec{v}_{part} = \frac{1}{B}\hat{z} \times \nabla\phi \quad \nabla \cdot \vec{v}_{part} \neq 0$ due to curvature.

Neglecting inertia effects $\propto M_{imp}/Zm_i$: only lighter impurities.

Impurity density: $D(n_{imp}/B)/Dt = 0$: Total mixing :: $n_{imp} \propto B$ :: Curvature pinch (Naulin, PRE **71**, 015402 (2005))

Impurity Dynamics

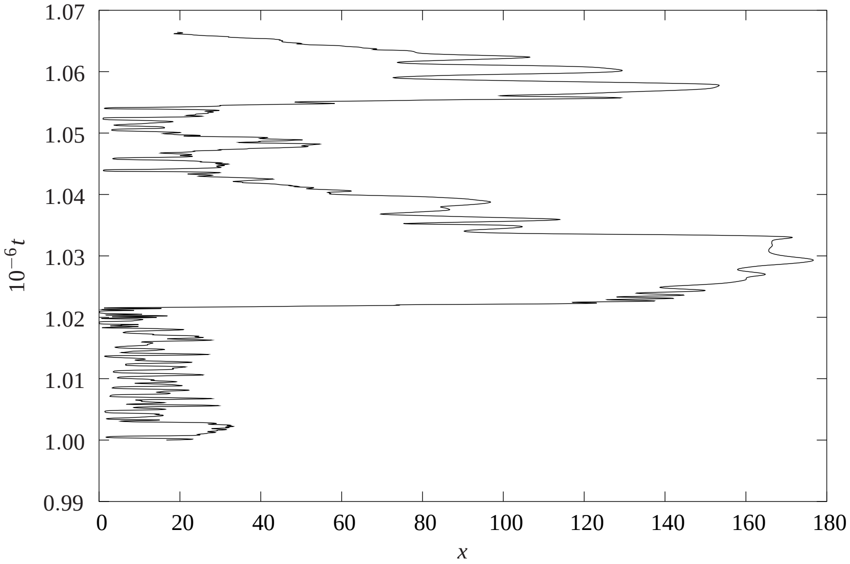

Trajectory of a test particle released inside LCFS

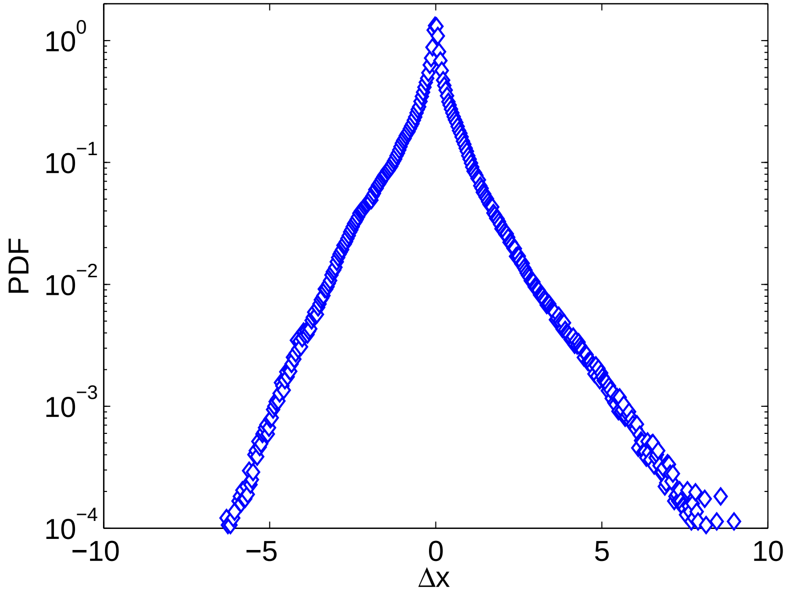

PDF of the radial displacement over $\Delta t = 50$ *Fat exponential tail!*

Impurity Dynamics

Impurity density: $D(n_{imp}/B)/Dt = 0$: Total mixing :: $n_{imp} \propto B$ :: Curvature pinch (Naulin, PRE **71**, 015402 (2005))

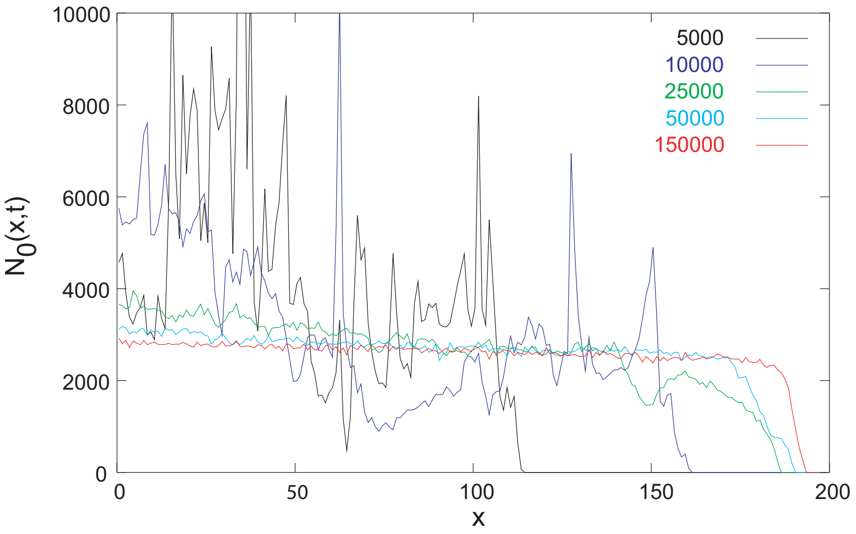

Distribution of impurities, that are initially released at x = 40, inside lcfs: Turbulent mixing.

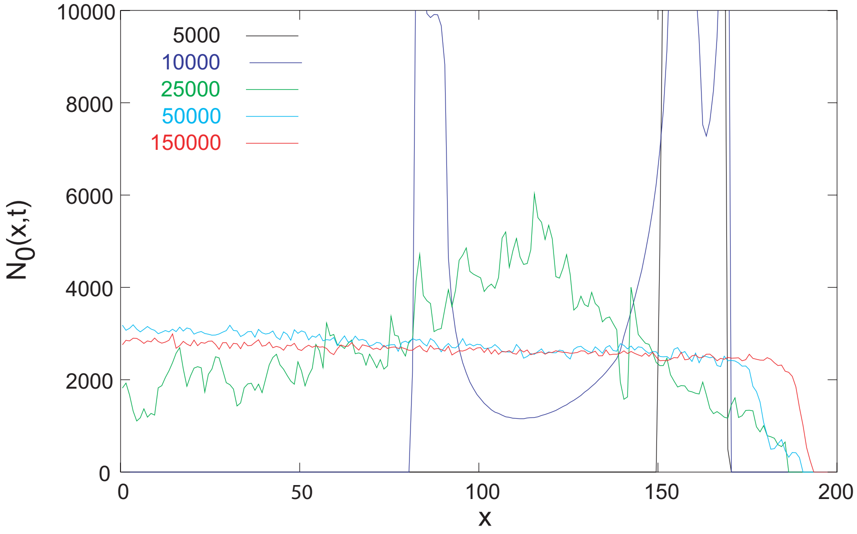

Distribution of impurities, that are initially released at x = 160: Turbulent mixing. Inward (curvature) pinch

Profiles

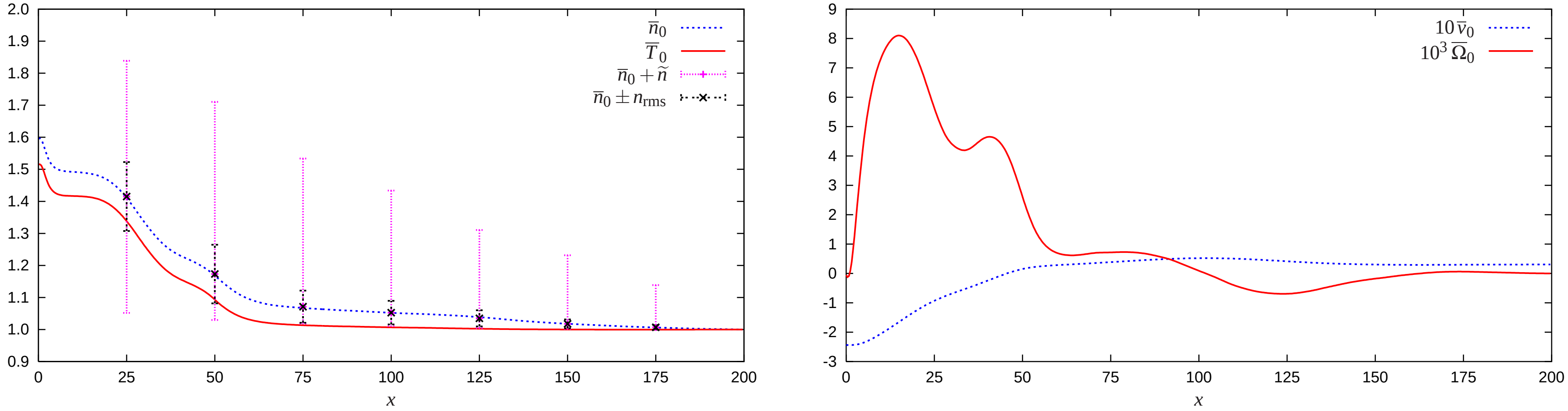

Time averaged profile of density, $\overline{n}_0$ *and temperature,* $\overline{T}_0$*: Strong gradients in the edge region (*$x < x_{LCFS} = 50$*) and flat profiles in the SOL.*

Time averaged profile of the poloidal flow, $\overline{v}_0$*,, and vorticity,* $\overline{\Omega}_0$ $(\nu = \times 10^{-2})$

Shear flow stabilization?

Influence of a background shear flow $V(x)\hat{y}$ on the classical interchange instability

Benilov *et al* Phys. Fluids **14** 1674 (2002)

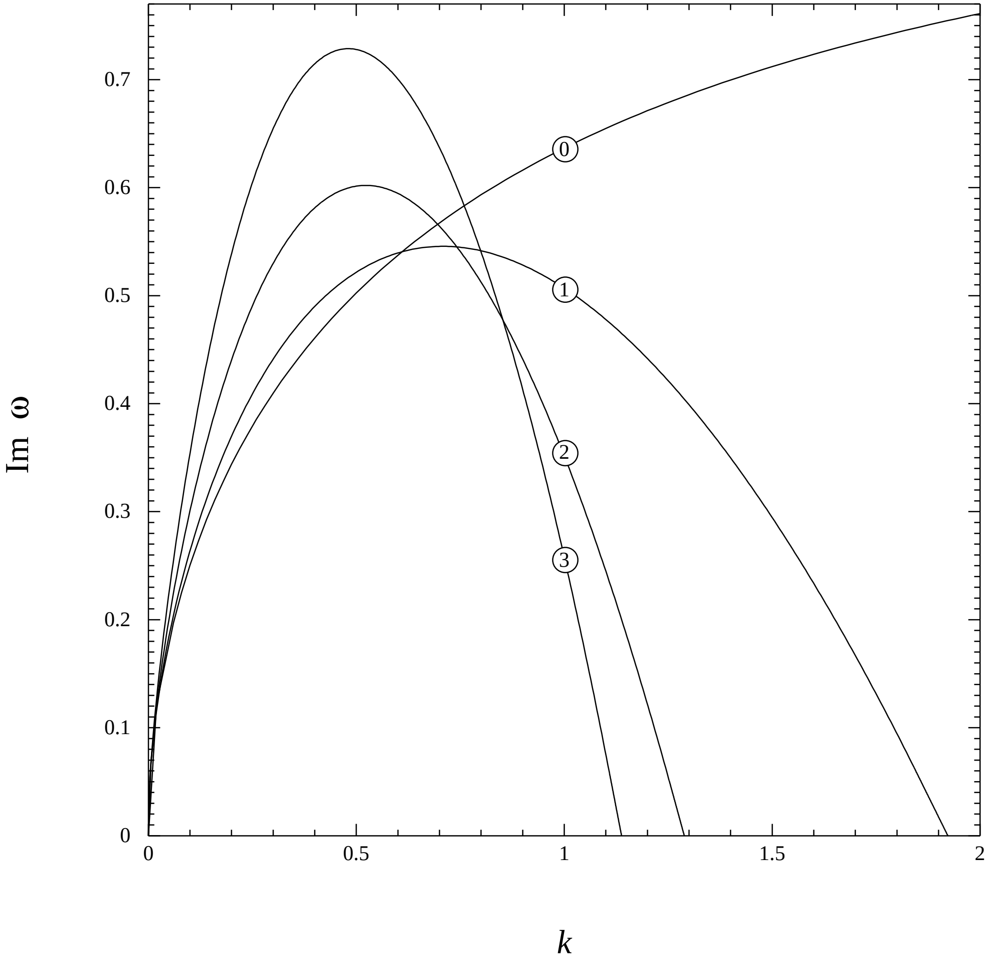

Numerical solution of linear dispersion relation: $V(x) = V_0 \tanh x$, $V_0 = 0,\ 0.5,\ 1.0,\ 2.0$

NOTE: Stability for $2\pi/L_y > k_c$